

## PHOTONS AND NEUTRAL MESONS FROM HOT HADRONIC MATTER\*

H. LÖHNER<sup>8</sup>, R. ALBRECHT<sup>1</sup>, T.C. AWES<sup>5</sup>, C. BARLAG<sup>4</sup>, F. BERGER<sup>4</sup>,  
M. BLOOMER<sup>2</sup>, C. BLUME<sup>4</sup>, D. BOCK<sup>4</sup>, R. BOCK<sup>1</sup>, D. BUCHER<sup>4</sup>,  
G. CLAESSON<sup>3</sup>, G. CLEWING<sup>4</sup>, R. DEBBE<sup>6</sup>, L. DRAGON<sup>4</sup>, A. EKLUND<sup>3</sup>,  
S. FOKIN<sup>7</sup>, S. GARPMAN<sup>3</sup>, R. GLASOW<sup>4</sup>, H.Å. GUSTAFSSON<sup>3</sup>, H.H. GUTBROD<sup>1</sup>,  
O. HANSEN<sup>6</sup>, G. HOELKER<sup>4</sup>, J. IDH<sup>3</sup>, M. IPPOLITOV<sup>7</sup>, P. JACOBS<sup>2</sup>,  
K.H. KAMPERT<sup>4</sup>, K. KARADJEV<sup>7</sup>, B.W. KOLB<sup>1</sup>, A. LEBEDEV<sup>7</sup>, I. LUND<sup>8</sup>,  
V. MANKO<sup>7</sup>, B. MOSKOWITZ<sup>6</sup>, F.E. OBENSHAIN<sup>5</sup>, A. OSKARSSON<sup>3</sup>,  
I. OTTERLUND<sup>3</sup>, T. PEITZMANN<sup>4</sup>, F. PLASIL<sup>5</sup>, A.M. POSKANZER<sup>2</sup>,  
M. PURSCHKE<sup>1</sup>, B. ROTERS<sup>1</sup>, S. SAINI<sup>5</sup>, R. SANTO<sup>4</sup>, H.R. SCHMIDT<sup>1</sup>,  
K. SÖDERSTRÖM<sup>3</sup>, S.P. SØRENSEN<sup>9</sup>, K. STEFFENS<sup>4</sup>, P. STEINHÄUSER<sup>4</sup>,  
E. STENLUND<sup>3</sup>, D. STÜKEN<sup>4</sup>, A. VINOGRADOV<sup>7</sup>, H. WEGNER<sup>6</sup>  
AND G.R. YOUNG<sup>5</sup>

<sup>1</sup> Gesellschaft für Schwerionenforschung (GSI), D-64220 Darmstadt, Germany

<sup>2</sup> Lawrence Berkeley Laboratory, Berkeley, California 94720, USA

<sup>3</sup> University of Lund, S-22362 Lund, Sweden

<sup>4</sup> University of Münster, D-48149 Münster, Germany

<sup>5</sup> Oak Ridge National Laboratory, Oak Ridge, Tennessee 37831, USA

<sup>6</sup> Brookhaven National Laboratory, Upton, New York 11973, USA

<sup>7</sup> Kurchatov Institute of Atomic Energy, Moscow 123182, Russia

<sup>8</sup> KVI, University of Groningen, NL-9747 AA Groningen, The Netherlands

<sup>9</sup> University of Tennessee, Knoxville, Tennessee 37996, USA

*(Received October 26, 1993)*

---

\* Presented at the XXIII Mazurian Lakes Summer School on Nuclear Physics, Piaski, Poland, August 18-28, 1993.

Results from the experimental program with light ion beams and heavy target nuclei at the CERN SPS could demonstrate the occurrence of an unprecedented state of high density in hadronic matter. The thermal nature of the hadronic system has been investigated by analyzing spectra and production ratios of hadrons which reveal a large degree of rescattering of primary and secondary hadrons. Thermal photons from elementary quark-gluon interactions are considered a promising signal for the occurrence of a phase transition to the quark-gluon plasma. The predictions for thermal photons from elementary parton interactions are discussed and compared to the thermal emission rate of photons from a hot hadronic gas. Recent results from the photon spectrometers in heavy ion experiments are presented. Production cross sections of  $\pi^0$  and  $\eta$  mesons are determined and the projectile and target mass dependence is discussed. An upper limit for the single photon yield was determined for central O+Au reactions. Recent S+Au reactions exhibit an excess of photons over the yield expected from hadronic decays. The spectral shape of the expected single photon signal is discussed which might reveal the temperature of hot matter and indicate a phase transition.

PACS numbers: 25.75. +r

## 1. Introduction

The study of the thermodynamic behaviour of a strongly interacting matter system will provide an interesting test of the confinement property of QCD. The interaction of elementary quark and gluon constituents is weakened by colour screening at very short distances. Sufficiently hot and dense matter should therefore become a gas of noninteracting quarks and gluons which move quasifreely in a deconfined but overall colour neutral environment given by the dimensions of the dense matter volume. Numerical simulations of statistical QCD [1–4] in the non-perturbative sector of QCD are very time-consuming calculations and still suffer from severe approximations. These refer to the quark-masses and the limited lattice size. The order of the phase transition is not firmly predicted. The required energy density is about  $1 - 3 \text{ GeV/fm}^3$  which is well above the energy density inside a single nucleon ( $\approx 0.5 \text{ GeV/fm}^3$ ). A transition temperature  $T_c \approx 160 \text{ MeV}$  appears to be a reasonable value [5] at zero baryonic chemical potential or zero baryonic density. This situation of purely mesonic matter might be accomplished in central collisions of heavy nuclei and observed in the phase space region around midrapidity ( $y_{\text{cm}} = 0$ ). The center-of-mass rapidity is defined as  $y_{\text{cm}} = \tanh^{-1}(\beta_{\parallel}^{\text{cm}})$ , with  $\beta_{\parallel}^{\text{cm}}$  the longitudinal particle velocity in the center-of-mass of the colliding nuclei.

The main experimental objective is to achieve a sufficiently large and long lived volume of matter close to thermal equilibrium at the required energy density. Further, multiple scattering of baryons and rescattering

of produced particles has to be demonstrated to ensure thermalization in hadronic matter. Finally, observation of real or virtual photons from elementary interactions of the matter constituents should allow to deduce the temperature evolution of the hot matter from the thermal emission rates. Photons are particularly suited, since their long mean free path leaves the photon signal free from distortions due to hadronic final state interactions. If quark matter has been produced in the course of the collision, a signal of colour deconfinement is expected from the spectroscopy of heavy quark bound states which would be suppressed due to colour screening [5].

In this lecture we discuss the experimental and theoretical investigations of real photon production in heavy ion reactions at SPS energies. Photons and neutral mesons have been measured in the WA80 [6, 7] experiment and with an upgraded setup in WA93. Lepton pairs, and thus photons through lepton pair conversion, have also been studied in the HELIOS [8] and CERES [9] experiments.

First we present the WA80 experiment. For the description of the experimental apparatus of other experiments we refer to the literature [10, 11]. Results from the recent heavy ion experiments giving indications for hot and dense hadronic matter will be summarized. Then we discuss the theoretical investigations of the various sources of photons in nuclear collisions at high energies. Next we introduce the experimental work on the single photon analysis and present results on the photon signal compared to theoretical expectations. We close with an outlook to the forthcoming Pb+Pb experiments.

## 2. The WA80 experimental setup

The WA80 experiment served the purpose to study global characteristics of heavy ion reaction events, and to investigate the momentum distributions of photons and neutral mesons in the high particle multiplicity environment at midrapidity. The setup shown in Fig. 1 combines an almost full coverage for charged particles with a calorimetric measurement of the energy flux at midrapidity, in the target-fragmentation region and at zero degrees. Details of the detection equipment are described in Refs [12–14].

For the spectroscopy of photons a lead glass array of 3800 detector elements is employed and arranged in 3 sections. The detector design follows closely the original photon detector of WA80 [14]. Photons are measured in a rapidity range  $2.1 \leq y_{\text{lab}} \leq 2.9$  for 60% of the full azimuthal ring around the beam direction. Charged particle rejection is achieved by two layers of streamer tube arrays [13] with an overall efficiency of 98%.

Neutral pions and  $\eta$  mesons are identified by their decay photons ( $\pi^0, \eta \rightarrow 2\gamma$ ). Transverse momentum ( $p_T$ ) distributions are obtained from

# WA80

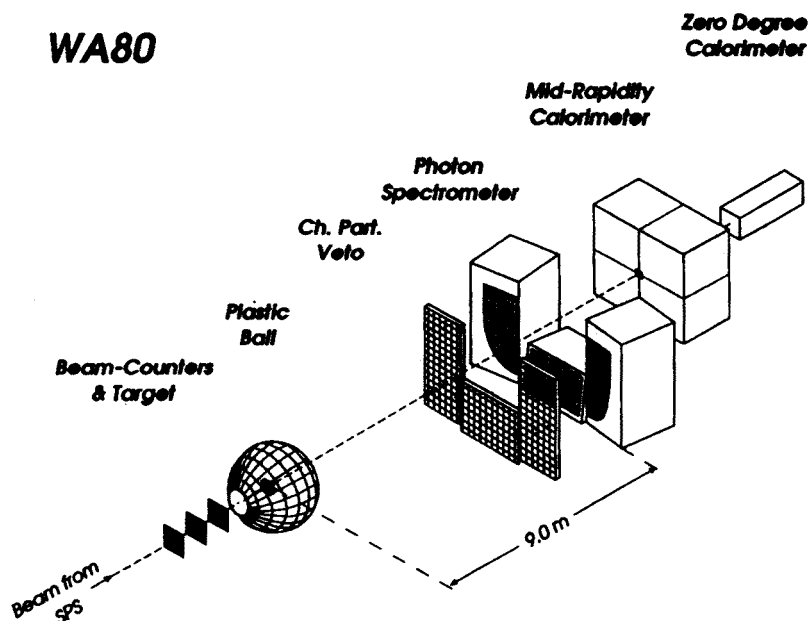


Fig. 1. The setup of the WA80 heavy ion experiment at the CERN SPS.

the meson yield as extracted from the invariant mass spectra. The meson efficiency depends sensitively on the signal/background ratio and the accurate subtraction of the combinatorial background which is due to unavoidable false pair combinations. An improved and fast photon and hadron identification method has been developed recently [15]. The precise shape of the combinatorial background is determined from polynomial fits to the invariant mass spectra. For unfavorably small signal/background ratios, dominantly at low transverse momenta, the mixed events method has proven to be a very powerful tool [16]. Finally, the obtained meson momentum distributions are corrected for the photon reconstruction efficiency and the geometrical acceptance obtained by a Monte Carlo calculation.

### 3. Indications for hot and dense matter

The degree of excitation of hot hadronic matter is characterized by the amount of energy deposited in the volume of interacting target and projectile nucleons, the energy density  $\epsilon_0$ . The energy density can be derived from final state observables under assumptions on the reaction geometry and the kinematical evolution. In order to estimate the uncertainty, extreme cases have been considered. In the partial stopping regime [17] at SPS energies the longitudinal growth of the reaction volume dominates the transverse expansion. Therefore, the transverse size of the reaction volume is given by

the projectile area  $\pi R_A^2$  while the longitudinal extension of a unit volume for the calculation of energy concentration is determined by the formation time  $\tau_0$ , the time needed before excited quark-objects appear as hadrons on the mass shell and interact with hadronic cross section. The energy density is given by the mean transverse energy per unit rapidity at midrapidity. These data are shown in Fig. 2 for different selections of impact parameters as defined experimentally by different amounts of missing forward energy which thus must appear at midrapidity. The marked maximum of  $\approx 100$  GeV per unit rapidity corresponds to  $\epsilon_0 = 2$  GeV/fm<sup>3</sup> if free hydrodynamic expansion [18] is assumed as derived by Bjorken:

$$\epsilon_0 = \frac{\left( \frac{dE_T}{d\eta} \right)_{\max}}{\pi R_A^2 \tau_0}. \quad (1)$$

The formation time is assumed to be 1 fm/c. If entropy conservation is considered, then for an isentropically expanding quark-gluon system an upper limit of the energy density of 3 GeV/fm<sup>3</sup> is estimated for the SPS energy of 200 GeV/nucleon. In any case, the amount of energy stopping appears to be sufficient to create the conditions for a quark-gluon plasma transition if thermalization is taken for granted.

The momentum distributions of identified mesons are studied to obtain further insight in the interaction dynamics of produced particles. The comparison between O+nucleus or S+nucleus and p+nucleus spectra shows a systematic dependence on  $A$  similar to the nuclear enhancement observed earlier [19] in  $p + \text{nucleus}$  as compared to  $p + p$  cross sections (Cronin effect). The target dependence has been parametrized by

$$\frac{d\sigma}{dp_T}(p + A) = A^{\alpha(p_T)} \frac{d\sigma}{dp_T}(p + p) \quad (2)$$

with an empirical  $p_T$  dependent exponent,  $1 \leq \alpha(p_T) \leq 1.2$ , where  $\alpha = 1$  is the limit of mere superposition of independent nucleon nucleon collisions. An explanation for the power-law dependence on  $A$ , consistent with the experimental systematics, is multiple low momentum scattering of partons in the hadronic medium. Quantitative calculations have been carried out for  $p + A$  reactions [20]. The projectile dependence was found to follow a similar parameterization [21]. The cross sections of central and peripheral S + Au reactions have been compared to  $p + p$  data in a similar rapidity range near midrapidity. The  $\pi^0$  cross sections divided by the charged  $\pi$  cross sections from  $p + p$  reactions [22] are shown in Fig. 3. The ratio shows a marked increase at large  $p_T$  which is more pronounced for the central reactions. Here, the larger effective interaction volume leads to a stronger influence of multiple interactions.

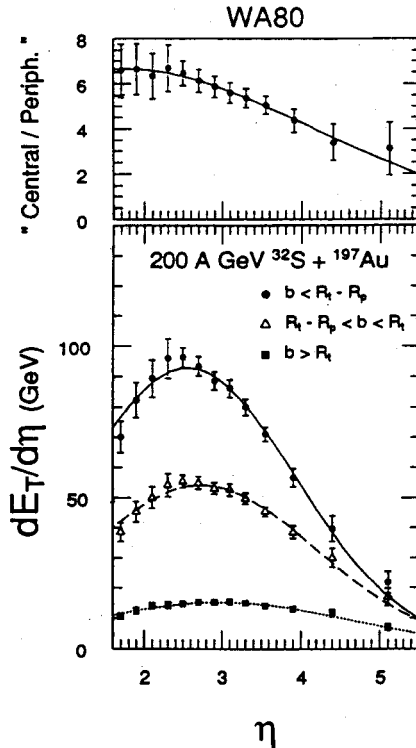


Fig. 2. (a) Measured transverse energy distribution for 200 GeV/nucleon S+Au reactions as function of the pseudorapidity  $\eta = -\ln \tan(\theta/2)$  for different estimated impact parameter ranges. The curves are gaussian fits to the data points. (b) The ratio of  $dE_T/d\eta$  distributions from central and peripheral reaction events.

Enhanced strangeness production with significant changes in the  $K/\pi$  ratios has been predicted as another signal for the quark-gluon plasma. The  $K/\pi$  ratios have been measured at BNL and SPS energies. A marked increase above the  $p+p$  level is observed for S+W reactions [23] in the range  $1 \leq y_{lab} \leq 1.5$  near the baryon rich target fragmentation region. The same increase in  $K^+/\pi^+$  from the  $p+p$  level to  $p$  + nucleus and nucleus+nucleus data is observed at the BNL energy. This suggests that rescattering is the responsible mechanism which may lead the heavy reaction system close to equilibrium.

An impressive set of data has been collected by the NA38 collaboration on the production of  $J/\psi$  mesons in  $p$  + nucleus and nucleus + nucleus collisions as compared to  $p+p$  reactions [24]. Scattering and absorption in the initial and final state have been investigated and reveal significant influence on the production and propagation of  $J/\psi$  mesons in dense matter, such that the experimentally studied transverse momentum and energy-

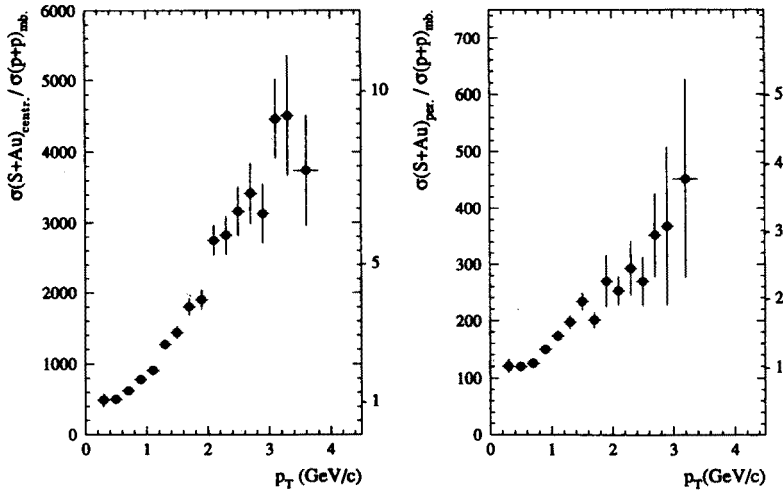


Fig. 3. Ratios of  $\pi^0$   $p_T$  distributions from central and peripheral S+Au reactions at 200 GeV/nucleon to charged  $\pi$  cross sections from p+p reactions.

density dependence can be explained. A spectral analysis of heavy quark bound states is proposed [5] to differentiate the deconfinement scenario from scattering and absorption in dense hadronic matter.

In summary, sufficient indications have been gathered in recent high energy heavy ion experiments for the existence of dense and highly excited hadronic matter. Interactions of hadrons are of significant influence to explain observed data so that approach to thermal equilibrium can be concluded. Direct observations of initial state features, unmodified by hadronic interactions, are thus desirable and expected from electromagnetic probes. Real photon production has been investigated. The photon yield should allow to draw a conclusion on the temperature of the emitting source.

#### 4. Sources of single photons

The emission rates of real photons and lepton pairs from virtual photon decay are a useful tool to study the interaction rate among constituents of matter investigated in high energy hadronic or nuclear collisions. Since the mean free path of electromagnetically interacting probes is much larger than the transverse size of colliding nuclei, the signal may be observed undisturbed by final state interactions.

##### 4.1. Photons from hard parton scattering

The production of high energy direct photons from large momentum transfer hadron-hadron collisions has been studied extensively [25, 26]. In

the first stage of a hadronic collision photons are produced in elementary interactions of valence and sea quarks. Their distribution is described by the structure functions giving the probability of finding a parton  $a$  in a hadron  $A$  with a fraction of the hadron momentum. The elementary parton subprocesses for high  $p_T$   $\gamma$  production are calculated in lowest order perturbation theory. These are the "QCD-Compton" process  $qg \rightarrow q\gamma$  and the annihilation  $q\bar{q} \rightarrow g\gamma$  which are of order  $\alpha\alpha_S$  in electromagnetic and strong coupling. Higher order terms like bremsstrahlung and soft gluon corrections are found to be important.

Information on the importance of gluon contributions to the structure functions could thus be obtained. The ratio  $\gamma/\pi^0$  increases with  $p_T$  since hadrons originate from jet fragmentation and receive a momentum fraction while photons carry essentially all the final state momentum of the partonic subprocess. On the other hand, extrapolating the hard scattering  $\gamma$  production to small momentum transfer  $Q^2$  in the thermal regime at low  $p_T \approx 1$  GeV/c, where no rigorous calculations are available yet, we expect a contribution of  $\gamma/\pi^0 \approx 0.01$ .

#### 4.2. Photons from the quark-gluon plasma

If high energy nuclear collisions lead to formation of a quark-gluon plasma the emission rate of photons from parton interactions in a thermal environment may provide information on the temperature of the system [28]. The calculations proceed in analogy to those introduced in the previous section. Instead of the structure functions the thermal distribution functions of partons describe the momentum spectrum of elementary interacting constituents. However, low  $Q^2$  processes have to be considered which are complicated by infrared divergences.

Recently, the resummation method for finite temperature perturbation theory [29] was applied to real photon production [30, 31]. The quark mass singularity is dynamically screened by many-body effects: One-loop corrections to the photon self-energy are calculated in the high temperature limit with effective (dressed) quark propagators. An analytic result for the photon rate at temperature  $T$  is obtained for the sum of annihilation and Compton contributions:

$$E_\gamma \frac{d^3 R_\gamma}{d^3 p_\gamma} = C \left( \sum_{n_f} e_q^2 \right) \frac{\alpha\alpha_S}{2\pi^2} T^2 e^{-E_\gamma/T} \left( \kappa_1 + \ln \frac{\kappa_2 E_\gamma}{\alpha_S T} \right) \quad (3)$$

with  $C = 1$ ,  $\kappa_1 = 0$  and  $\kappa_2 = 0.23$ . Various approximations [32–34] have been used which lead to a similar analytic dependence on  $E_\gamma$  and  $T$  but differ in the constants  $\kappa_1$  and  $\kappa_2$ , and in the absolute normalization  $C$ . Results of different evaluations at a temperature  $T = 200$  MeV are compiled



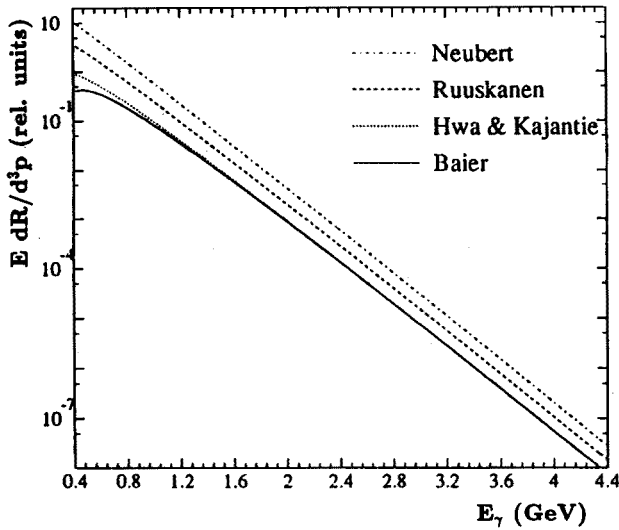


Fig. 4. Calculated thermal photon emission rates for different theoretical approaches at a temperature of 200 MeV.

in [35] and compared in Fig. 4 in the photon energy range where the high temperature approximation gives reliable results. The thermal propagator approach of Baier gives about a factor 5 lower photon rates than the evaluation of Neubert, where many-body screening effects were not taken into account.

#### 4.3. Photons from hot hadronic matter

If nuclear collisions lead to the formation of hot hadronic matter, then photon emission from the electromagnetic coupling of interacting mesons (dominantly  $\pi^\pm$ ) needs to be taken into account. The relevant processes have been studied recently [30]. Annihilation and Compton processes were considered among which  $\pi\pi \rightarrow \rho\gamma$  dominates at small photon energies and  $\pi\rho \rightarrow \pi\gamma$ , with higher available energy due to the  $\rho$  mass in the initial state, contributes most in the tail of the photon spectrum. With thermal momentum distribution functions at temperature  $T$  the hadronic collisions give rise to similar photon rates as expected from parton interactions at the same temperature. The importance of the  $A_1(1260)$  resonance formation in the process  $\pi\rho \rightarrow A_1 \rightarrow \pi\gamma$  has been pointed out [36] with a photon rate competing with hadron scattering.

Thus a photon signal is expected even if the plasma phase has not been reached. Since the hadronic matter phase is expected to dominate at a lower temperature over the quark-gluon plasma, the spectral shape of the photon signal needs to be analysed and should allow to separate the different contributions.

### 5. Space-time evolution

In order to evaluate the photon yield that can be compared to experimental data the space time evolution of the interacting system needs to be considered. The reaction volume develops from proper time  $\tau=0$ , when projectile and target nuclei overlap, to maximum energy density in a highly excited and thermalized stage at  $\tau_1$  with initial temperature  $T_i(\tau_1)$ . Subsequently, the system cools down to the freeze-out temperature  $T_f(\tau_f)$  where interactions cease. A first-order phase transition at the critical temperature  $T_c$  might lead to an extended mixed phase. The expected temperature profile will influence considerably the photon yield so that estimates for the space time evolution are highly desirable. Various attempts based on hydrodynamical expansion and an ideal gas equation of state have been made [32, 37, 38].

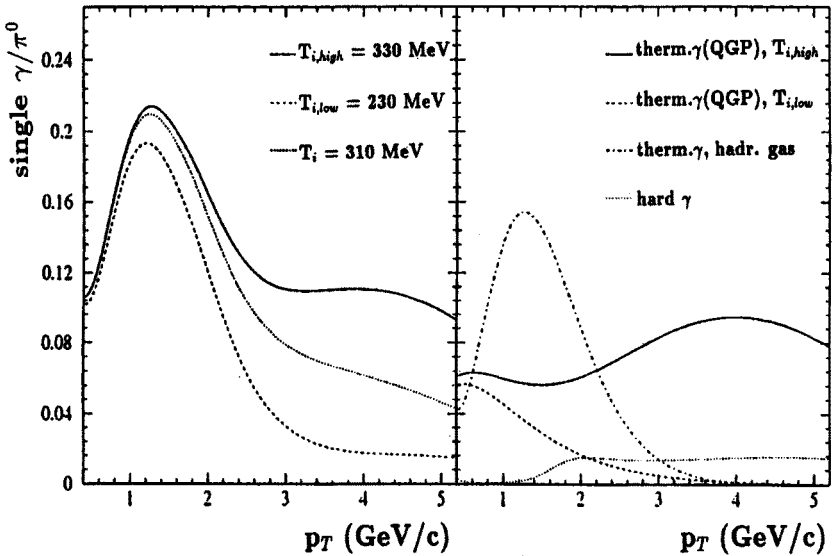


Fig. 5. The calculated  $\gamma/\pi^0$  ratio based on a dynamical situation as expected for 200 GeV/nucleon S+Au reactions for different initial temperatures and a critical temperature of 160 MeV.

Hydrodynamical model calculations have been applied to describe the expansion scenario which proceeds isentropically and is dominated by longitudinal expansion. The space-time integration was carried out [35], based

on the photon rate calculated in [34], in order to obtain the photon yield

$$E_\gamma \frac{d^3 \sigma_\gamma}{d^3 p_\gamma} = \int_{\tau_i}^{\tau_f} d\tau dy \tau \kappa R_A^2 E_\gamma \frac{d^3 R_\gamma(T(\tau))}{d^3 p_\gamma}, \quad (4)$$

in the rapidity interval  $dy$  at midrapidity. Results from these calculations for different initial temperatures  $T_i$  and  $T_c = 160$  MeV are shown in Fig. 5, where photon cross sections have been divided by the measured  $\pi^0$  production cross section at the corresponding  $p_T$ . The summed production yield of all photon processes discussed earlier peaks slightly above  $p_T = 1$  GeV/c with significant differences at large  $p_T$  for different initial temperatures. A considerable yield above the currently achievable detection limit of  $\gamma/\pi^0 \approx 0.05$  may then be expected. Looking at the individual contributions to the photon yield, the yield from the hadron phase clearly dominates at low  $p_T$  and the relatively low initial temperatures expected for the S+Au reactions at SPS energies. Photons from hard parton scattering stay below  $\gamma/\pi^0 \approx 0.02$  in the photon energy range currently accessible by experiment and thus below the detection limit.

## 6. Single photon analysis

The measured momentum distributions of  $\pi^0$  mesons and the determination of the  $\eta/\pi^0$  production ratio provide the basis for extracting the rate of single photons from the measured inclusive photon yield. Severe problems arise from the high particle multiplicity and the tremendous hadronic background of photons from neutral meson decays. The single photon to  $\pi^0$  ratio ( $\gamma/\pi^0$ ) is calculated from the total measured photon yield  $N_\gamma$  and the measured pion yield  $N_{\pi^0}$  according to the following expression:

$$\frac{\gamma}{\pi^0} = \frac{N_\gamma}{N_{\pi^0}} \frac{\epsilon_{\pi^0}}{\epsilon_\gamma} A_{\text{geo}} - (R_{\pi^0} + R_\eta + R_x). \quad (5)$$

The  $\epsilon_{\pi^0}$  and  $\epsilon_\gamma$  are the  $\pi^0$  and photon reconstruction efficiencies, respectively,  $A_{\text{geo}}$  is the geometrical acceptance of the detector for  $\pi^0$  and the  $R_i$  are the Monte Carlo calculated ratios of observed background photon yield from meson decays to the detected  $\pi^0$  yield for each of the sources  $i$ . Besides photons originating from  $\pi^0$  and  $\eta$  decays we also take into account the decays of  $\eta'$ ,  $\omega$ ,  $\phi$ ,  $K^0$  and  $\Sigma^0$  with contributions well below that from the  $\eta$  mesons. Measured  $p_T$  distributions for  $\pi^0$  [6] and  $\eta$  mesons are the basis for the Monte Carlo background calculation. The non-measured resonance

decays contribute only  $\approx 2\%$  to the photon background and are based on p+p data and scaling [39] with the transverse mass  $m_T = \sqrt{p_T^2 + m^2}$  as:

$$f(m_T; h) = C f(m_T; \pi^0); \quad h = \eta, \eta', \omega. \quad (6)$$

The  $\eta$  production is measured with the photon detector array exploiting the 38.9% branch into the  $\gamma\gamma$  decay channel. For 200 GeV/nucleon O+Au reactions a value  $\eta/\pi^0 = 0.61 \pm 0.2$  was measured for minimum-bias reactions in the  $p_T$  region  $2 \text{ GeV}/c \leq p_T(\gamma\gamma) \leq 2.4 \text{ GeV}/c$ . This ratio is consistent with the  $\eta/\pi^0$  ratio from  $p + p$  reactions. For the analysis of recent S+Au data the mixed events method to subtract the combinatorial background was developed and tuned to simulated data [16, 40, 41]. The  $\eta$  cross sections for S+Au reactions, as measured in the range  $0.5 \text{ GeV}/c \leq p_T(\gamma\gamma) \leq 2.5 \text{ GeV}/c$ , are shown in Fig. 6 together with the  $\pi^0$  results. The momentum distributions are parametrized by the following expression [42]:

$$E \frac{d^3\sigma}{d^3p} = C \left( \frac{p_0}{p_T + p_0} \right)^n, \quad (7)$$

with free parameters  $C$ ,  $p_0$  and  $n$ . The power-law ansatz is deduced in a model of hard collisions of quarks based on QCD. Transformed into the  $m_T$  scale, the resulting fit is included in Fig. 6. Except for the absolute normalization, the same parameters also fit the  $\eta$  distribution, so that a ratio  $\eta/\pi^0 = 0.61 \pm 0.08$  is obtained for the minimum-bias S+Au data.

## 7. Results on single photons

Since the transition to a quark-gluon plasma state and hence an excess of single photons is expected to occur more likely in central than in peripheral reactions, the 200 GeV/nucleon S+Au data sample has been divided into peripheral and central events. This selection was made according to the transverse energy measured in the midrapidity calorimeter and results are shown in Fig. 7. The circles indicate the experimental inclusive photon yield and the histograms are Monte Carlo results based on the measured  $\pi^0$  and  $\eta$  yield and represent the hadronic background. A difference between experimental inclusive photon yield and the histograms must be attributed to the contribution of single photons. The general  $p_T$  dependence of the data is well reproduced by the Monte Carlo simulations.

The central S+Au data show a slight overall enhancement over the hadronic background. Collecting all sources of statistical and systematic errors and assuming them to follow a gaussian distribution, we arrive at an uncertainty of 6–8% and 8–15% for  $p_T$  bins below and above 2 GeV/c, respectively. The excess of photons in central data over the expected yield

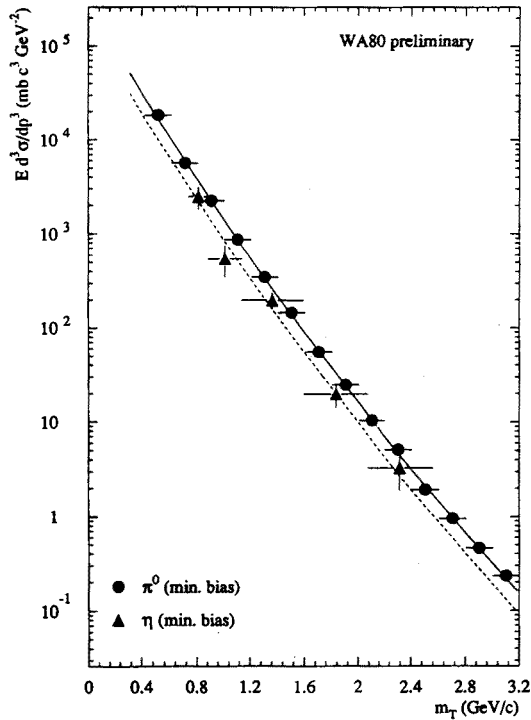


Fig. 6. The invariant cross sections for  $\pi^0$  and  $\eta$  mesons as function of the transverse mass  $m_T$  for minimum bias reactions of S+Au at 200 GeV/nucleon.

from the hadronic background observed for  $p_T < 2 \text{ GeV}/c$  reaches a level of 2 standard deviations [40, 43].

The remaining single photon yield, obtained by subtracting the calculated decay contribution from the inclusive photon yield, is shown in Fig. 8 for central S+Au reactions. Contrary to the peripheral data, the central sample shows a positive signal and a slight increase towards low  $p_T$ . This feature resembles the spectral shape expected from hadronic interactions at a temperature below 200 MeV/c.

Inclusive photon production has also been studied by the NA34 collaboration [8] for O+W data. The inclusive photon results are compatible with the expectations from hadronic decays. Recent data from the NA45-CERES dilepton spectrometer [9] could provide a single photon estimate of  $\gamma/\pi^0 = 0.08 \pm 0.11$  averaged in the range  $0.4 \text{ GeV}/c \leq p_T \leq 2.4 \text{ GeV}/c$  for S+W reactions.

At this stage of the data analysis, however, no quantitative comparison to calculated photon spectra will be made. This is because large uncertainties in the estimation of the initial conditions allow only rough predictions. The experimental analysis is extremely tedious due to critical Monte Carlo

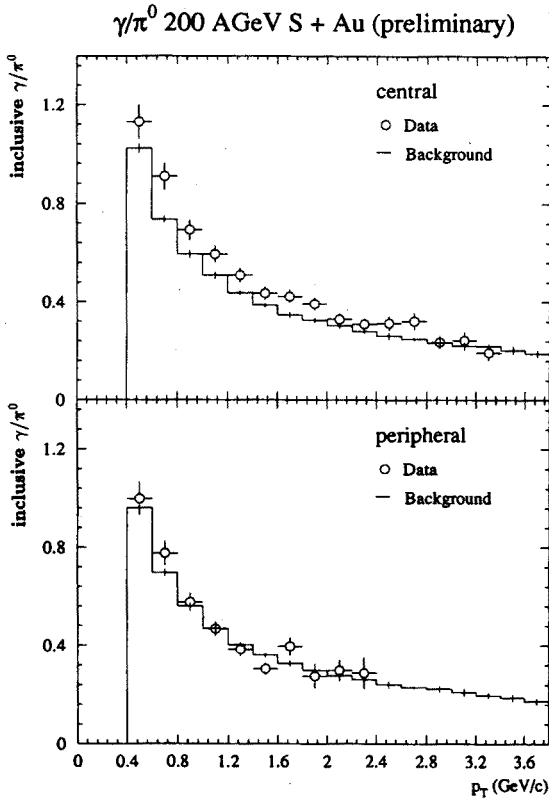


Fig. 7. Ratio of the inclusive photon cross section to  $\pi^0$  cross section as a function of transverse momentum for central and peripheral S+Au reactions at 200 GeV/nucleon. The circles indicate the data, and the histograms are the Monte Carlo results representing the hadronic decay background.

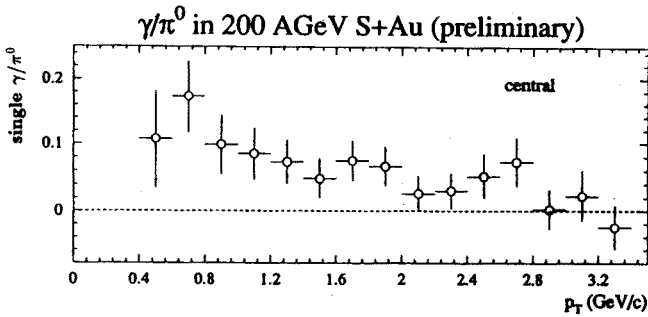


Fig. 8. Single photon yield for central S+Au reactions at 200 GeV/nucleon. The data are obtained by subtracting the Monte Carlo calculated hadronic decay background from the inclusive  $\gamma/\pi^0$  spectrum as shown in Fig. 7.

procedures in the determination of the photon and  $\pi^0$  efficiency. Therefore an independent re-analysis is planned in order to gain extra confidence in the estimates of systematic errors. The measured photon yield could then be used to estimate the hadronic temperature from the low  $p_T$  yield and to set limits on the contribution from a high temperature quark-gluon plasma phase at high  $p_T$ .

## 8. Outlook to forthcoming experiments

New experiments are being planned at the CERN SPS for the near future. For the first time, Pb ions will be accelerated to 160 GeV/nucleon. In Pb+Pb collisions at this energy interactions volumes above 7000 fm<sup>3</sup> are likely [5] so that truly thermal behaviour of hot hadronic matter may be expected. The  $A$  dependence of the thermalization time could lead to an initial temperature as high as 400 MeV so that the photon yield from the quark-gluon plasma at large  $p_T$  is quite prominent. The spectral shape of the photon yield could thus not only provide the temperature of the emitting system but also might indicate a possible phase change and reveal the critical temperature from the low  $p_T$  photon yield.

Recently, photon intensity interferometry has been studied theoretically [44]. The correlation functions reflect the different time scales of the system in the plasma, hadronic or mixed phase. Since photons from the plasma phase dominate at high  $p_T$ , the correlation functions for high  $p_T$  photons are found to be sensitive to the space-time evolution of the quark-gluon plasma.

The largely extended WA80 photon detector will be implemented in the WA98 setup for Pb+Pb collisions. About 10000 Pb-glass elements might provide sufficient spatial resolution to investigate photon correlations experimentally. A photon multiplicity detector is included to allow selection of photon-rich events. Charged hadrons will be measured in a dipole spectrometer, so that electromagnetic and hadronic signals can be correlated. In this way, a sensitive selection of reaction events is expected that may reveal the quark-gluon plasma signature.

## 9. Summary

The thermal photon signal to reveal the quark-gluon plasma in high energy nuclear collisions has been investigated theoretically and experimentally. Central reaction events exhibit an energy density of about 4 times the energy density inside a single nucleon. A large degree of rescattering of primary and secondary hadrons can explain the measured  $K^+/\pi^+$  ratio and

the suppression of the  $J/\psi$  production in central collisions. Rescattering is a prerequisite to achieve thermalization.

Calculations of single photon production from various sources have been reviewed. Photons from hot hadronic matter occur at the same rate and exhibit a similar spectral shape as photons from the quark-gluon plasma at the same temperature. Within a hydrodynamical scenario, the space-time evolution of hot matter is discussed and the photon yield is calculated by integration over the temperature evolution.

Experimental data reveal for the first time an excess of single photons above the yield expected from hadronic decay sources. The spectral shape suggests photon emission from hot hadronic matter.

Results presented in this work are based to a large extent on thorough experimental investigations conducted by the photon teams at Univ. Münster and the Kurchatov Institute Moscow. Inspiring discussions with Prof. R. Santo, Dr. K.H. Kampert, Dr. G. Clewing, G. Hölker and D. Bucher are gratefully acknowledged. This work was supported in part by the German BMFT and DFG, the United States DOE, the Dutch Foundation FOM, the Swedish NFR, and the CERN PPE division.

## REFERENCES

- [1] H. Satz, *Ann. Rev. Nucl. Part. Sci.* **35**, 245 (1985).
- [2] F. Karsch, R. Petronzio, *Z. Physik* **C37**, 627 (1988).
- [3] J. Engels *et al.*, *Phys. Lett.* **B252**, 625 (1990).
- [4] F.R. Brown *et al.*, *Phys. Rev. Lett.* **65**, 2491 (1990).
- [5] H. Satz, CERN-TH.6666/92 preprint and BI-TP 92/37 preprint.
- [6] R. Albrecht *et al.*, WA80 Collaboration, *Z. Phys.* **C47**, 367 (1990).
- [7] R. Albrecht *et al.*, WA80 Collaboration, *Z. Phys.* **C51**, 1 (1991).
- [8] T. Åkesson *et al.*, NA34/HELIOS Collaboration, *Z. Phys.* **C46**, 369 (1990).
- [9] A. Drees, NA45/CERES Collaboration, invited talk presented at the Tenth International Conference on Ultra-Relativistic Nucleus-Nucleus Collisions, Borlänge, Sweden 1993, to be published in *Nucl. Phys. A*.
- [10] H.R. Schmidt, J. Schukraft, GSI preprint GSI-92-19, to be published in *J. Mod. Phys. G*.
- [11] J. Stachel, G.R. Young, *Ann. Rev. Nucl. Part. Sc.* Vol. **42**, 537 (1992).
- [12] G.R. Young *et al.*, *Nucl. Instr. Meth.* **A 279**, 503 (1989); T.C. Awes *et al.*, *Nucl. Instr. Meth.* **A279**, 479 (1989).
- [13] R. Albrecht *et al.*, *Nucl. Instr. Meth.* **A 276**, 131 (1989).
- [14] H. Baumeister *et al.*, *Nucl. Instr. Meth.* **A292**, 81 (1990).
- [15] F. Berger *et al.*, *Nucl. Instr. Meth.* **A321**, 152 (1992).
- [16] S. Lebedev, WA80 Collaboration, invited talk presented at the Tenth International Conference on Ultra-Relativistic Nucleus-Nucleus Collisions, Borlänge, Sweden 1993, to be published in *Nucl. Phys. A*.



- [17] R. Albrecht *et al.*, WA80 Collaboration, *Phys. Rev.* **C44**, 2736 (1991).
- [18] J.D. Bjorken, *Phys. Rev.* **D27**, 140 (1983).
- [19] J.W. Cronin *et al.*, *Phys. Rev.* **D11**, 3105 (1975); D. Antreasyan *et al.*, *Phys. Rev.* **D19**, 764 (1979).
- [20] M. Lev, B. Petersson, *Z. Phys.* **C21**, 155 (1983).
- [21] T. Åkesson *et al.*, NA34/HELIOS Collaboration, *Z. Phys.* **C46**, 361 (1990).
- [22] B. Alper *et al.*, BS Collaboration, *Nucl. Phys.* **B100**, 237 (1975).
- [23] H. van Hecke *et al.*, NA34 Collaboration, *Nucl. Phys.* **A525**, 227c (1991); T. Åkesson *et al.*, NA34/HELIOS Collaboration, *Phys. Lett.* **B296**, 273 (1992).
- [24] C. Baglin *et al.*, NA38 Collaboration, *Phys. Lett.* **B251**, 465 (1990).
- [25] T. Ferbel, W.R. Molzon, *Rev. Mod. Phys.* **56**, 181 (1984).
- [26] J.F. Owens, *Rev. Mod. Phys.* **59**, 465 (1987).
- [27] E. Anassontzis *et al.*, *Z. Phys.* **C13**, 277 (1982); A.P. Contogouris, S. Papadopoulos, J. Ralston, *Phys. Rev.* **D25**, 1280 (1982).
- [28] E.L. Feinberg, *Nuovo Cimento* **34A**, 391 (1976).
- [29] N.P. Landsman, Ch.G. van Weert, *Phys. Rep.* **145**, 141 (1987).
- [30] J. Kapusta, P. Lichard, D. Seibert, *Phys. Rev.* **D44**, 2774 (1991).
- [31] R. Baier, H. Nakkagawa, A. Niegawa, K. Redlich, *Z. Phys.* **C53**, 433 (1992).
- [32] M. Neubert, *Z. Phys.* **C42**, 231 (1989).
- [33] R.C. Hwa, K. Kajantie, *Phys. Rev.* **D32**, 1109 (1985).
- [34] P.V. Ruuskanen, *Nucl. Phys.* **A544**, 169c (1992); K. Kajantie, P.V. Ruuskanen, *Phys. Lett.* **B121**, 352 (1983).
- [35] D. Bucher, Diploma thesis, Univ. Münster 1993.
- [36] L. Xiong, E. Shuryak, G.E. Brown, *Phys. Rev.* **D46**, 3798 (1992).
- [37] S. Chakrabarty *et al.*, *Phys. Rev.* **D46**, 3802 (1992).
- [38] D. Seibert, *Z. Phys.* **C58**, 307 (1993).
- [39] J. Bartke *et al.*, *Nucl. Phys.* **B120**, 14 (1977); E.V. Shuryak, *Phys. Rep.* **61**, 71 (1980).
- [40] G. Clewing, PhD thesis, Univ. Münster 1993.
- [41] G. Hölker, PhD thesis, Univ. Münster 1993.
- [42] R. Hagedorn, *Rivista del Nuovo Cimento* Vol. **6**, 1 (1983).
- [43] R. Santo, WA80 Collaboration, invited talk presented at the Tenth International Conference on Ultra-Relativistic Nucleus-Nucleus Collisions, Borlänge, Sweden 1993, to be published in *Nucl. Phys. A*; IKP-MS-93/0701 preprint 1993.
- [44] D.K. Srivastava, J.I. Kapusta, *Phys. Lett.* **B307**, 1 (1993).